

# Effect of the Temperature on the Nonlinear Acoustic Behavior of Reinforced Concrete Using Dynamic Acoustoelastic Method of Time Shift

Farid Moradi-Marani · Serge Apedovi Kodjo ·  
Patrice Rivard · Charles-Philippe Lamarche

Received: 30 September 2013 / Accepted: 17 December 2013 / Published online: 28 January 2014  
© Springer Science+Business Media New York 2014

**Abstract** During field tests, there is almost no effective way to control thermal changes in concrete structures. It is obvious that temperature fluctuations influence nonlinear acoustic behavior of concrete, which may lead to incoherent results during field investigations. The research presented herein was conducted to assess the effects of temperature changes on the nonlinear acoustic behavior of the reinforced concrete using Time Shift method. The Time Shift method, based on dynamic acoustoelastic principle, takes its roots from the coda wave interferometry method and combines it with the study of the nonlinear behavior in cementitious materials in a methodological manner that allows field investigations. Near-to-field environmental conditions were simulated in the laboratory using an automatic climatic room. The specimens were subjected to temperature changes ranging from  $-10$  to  $40$  °C. Such a thermal regime is close to the thermal conditions prevailing for most concrete structures. The effect of the temperature variations was assessed in both sound and damaged concrete elements affected by alkali–silica reaction (ASR). The test-results demonstrate that the nonlinear acoustic responses of concrete depend on the temperature. However, the nonlinear parameter seems to get minimized in low temperatures ranging from  $-10$  to  $10$  °C. Moreover, the state of medium (i.e. intact or damaged) can alter the sensitivity level of the nonlinear behavior to temperature variations.

**Keywords** Nondestructive testing · Nonlinear acoustic · Dynamic · Temperature · Concrete · Alkali–silica reaction

---

F. Moradi-Marani (✉) · S. A. Kodjo · P. Rivard · C.-P. Lamarche  
Civil Engineering Department, Université de Sherbrooke,  
Sherbrooke, QC J1K 2R1, Canada  
e-mail: farid.moradi@usherbrooke.ca

## 1 Introduction

Recent research in the domain of civil engineering structures maintenance aims at developing damage detection methods by which maintenance measures become more cost-effective and more reliable. This can be achieved by the early detection of defects and deteriorations in structures. This approach is attracting much attention worldwide, especially for concrete structures in which the early recognition of inner degradations prior to their extension to surface is fairly hard to get. Finding appropriate methods to evaluate micro-damage at an early stage is one of the main challenges in health monitoring of concrete structures. Nonlinear acoustics (NLA) methods have been successful in finding small and micro-size defects in engineering materials [1,2]. However, limited research on NLA methods has been conducted for the monitoring of reinforced concrete [3]. The great sensitivity of the NLA methods to damage is helpful for evaluating concrete; nevertheless, the influence of the environmental parameters (e.g. water content, temperature) on the NLA properties of the concrete should be well understood in order to uncouple the influence of damage and the environmental parameters.

Unlike metals, concrete is a multiphase and inherently isotropic heterogeneous material, consisting of multiple scale components (e.g. cement particles and coarse/fine aggregates); pores; inherent micro-defects; as well as pore solution; and interlayer water which are randomly distributed in the matrix. Because of this inherent heterogeneity and scattering, the NLA response of the concrete is subjected to an alteration from the temperature. A phenomenological model, which has been quantitatively validated by Vakhnenko et al. [4], may describe the dependence of behavior of concrete to temperature and water saturation:

$$E = E_0 \left[ 1 - f(S, T) \left( 1 + \frac{\delta c}{c_0} \right) \right] \tag{1}$$

where  $E$  and  $E_0$  are nonlinear and linear modulus of elasticity, respectively;  $f(S, T)$  is an exponential function which is dependent on the water saturation ( $S$ ) and temperature ( $T$ );  $\delta c$  is the defect variation; and  $c_0$  is the initial defect concentration. It is inferred from this model that thermal dependency of NLA behavior of a medium can be intensified by damage propagation through the medium. Therefore, a damage mechanism like alkali–silica reaction (ASR) can increase the sensitiveness of the NLA behavior of the medium to variations of temperature.

Payan et al. [5] have studied the effect of the water saturation on the nonlinear elastic response changes in concrete blocks. Their results showed a sudden decrease of the NLA parameter from dry condition up to 20 % saturation, which was related to solid–fluid interactions. For saturation above 20 %, the capillary condensation dominated, and only negligible fluctuations were observed. This observation was qualitatively equivalent to that made for chalk specimens that were studied by Johnson et al. [6], and by Carmeliet and Abeele [7]. Indeed, the work presented by Payan et al. [5] demonstrated that water saturation is not as important as temperature variations when concrete structures are exposed to atmospheric conditions with water saturation between 30 and 100 %. In the field of acoustic testing, temperature changes at normal thermal regimes have been mostly considered for metallic structures [8–10]. A study, carried out by Darling et al. [11] for a wide range of temperature variations, demonstrated that the thermal variations affect the NLA response of earth materials. However, the effect of the temperature variations on NLA behavior of concrete, either sound or damaged, is yet more under question.

An approach based on the time shift of acoustic waves using dynamic acoustoelastic principle has been used in this paper in an attempt to determine the effect of temperature changes on the NLA behavior of reinforced concrete. The Time Shift method is recommended as a potentially suitable method for monitoring micro-damage in concrete structures [12]. The performance of this method developed by Kodjo [12] was assessed in a laboratory experimental research by Bui et al. [13]. Time Shift method is based on the perturbation of micro-defects/defects by high-amplitude pump waves, which are imposed by an instantaneous impulse loading (e.g. hammer strike), when the medium is simultaneously probed by weak amplitude—high-frequency waves. The time delay occurring in probe waves is directly correlated with NLA state of the medium.

This research was conducted in a simulated environmental condition in the laboratory using a controlled climatic room. Three reinforced concrete slabs were fabricated to perform experiments on sound and damaged concrete slabs. Damage

to concrete was created by incorporating reactive coarse aggregate in the concrete mixture. This procedure leads to a progressive expansion of the concrete and the formation of a crack network through the specimen. This harmful reaction is known as ASR and affects a large number of structures worldwide. The tests were performed in temperatures ranging between  $-10$  and  $40$  °C, which is representative of the ambient temperature found in most of urban areas, specifically in northern countries.

## 2 Theoretical Background

Time Shift method is based on the nonlinear acoustic response of materials and it aims at quantifying the damage level in continuous medium by measuring the delay of the arrival time of probe waves. The measured delays that are measured in the late arrival portions of probe waves (i.e. coda waves) are generally greater than those in the early arrival portions. In the case of micro-damage in heterogeneous materials (e.g. concrete), the travel time of the probe waves may remain unchanged unless the media is disturbed by an external mechanical perturbation. By applying a mechanical distribution such as an impact force, micro-cracks are excited (i.e. reversible deformations occur in micro-cracks) so the travel time of probe waves is altered. This alteration is computed when the probe waves before perturbations are compared with the waves following the perturbations in order to find the relative time shift related to the imposed excitations [13, 14].

The relative time shift ( $\Delta t/t_0$ ) and the relative velocity variation ( $\Delta V/V_0$ ) for the longitudinal probe waves can be associated with together; it should be mentioned that this association is directly proportional to the nonlinearity of the materials. To calculate this variation, two important assumptions are considered during each test: (1) if the medium is perturbed by a mechanical impact, no significant changes occur in the path of the probe waves; and (2) the geometrical dimensions of the tested medium should remain constant. In the physic of wave propagation, the time travel of a simple longitudinal P-wave of constant velocity  $V_0$  in a medium at rest is defined by the equation of motion  $t_0 = \frac{1}{V_0} \int_L dx$ . When a low-amplitude probe signal propagates through a medium disturbed by high-amplitude perturbations (e.g. mechanical impact), the constant average velocity of the waves  $V$  changes to  $V + \Delta V$ . Assuming that the relative velocity ratio  $\Delta V/V_0$ , from the undisturbed state to the disturbed state remains independent of all possible paths of travel; the travel time in the disturbed medium is:

$$t_0 + \Delta t = \frac{1}{V_0 + \Delta V} \int_L dx = \frac{V_0 - \Delta V}{V_0^2 - \Delta V^2} \int_L dx \tag{2}$$

where  $\Delta t$  is the *time shift*, which corresponds to the difference in travel time between the disturbed and undisturbed medium scenarios. Equation 1 can be rewritten:

$$t_0 + \Delta t = \left( \frac{1}{V_0} - \frac{\Delta V}{V_0^2} \right) \int_L dx \tag{3}$$

Because  $\Delta V^2$  is a second order term that tends toward zero, and replacing  $t_0 = \frac{1}{V_0} \int_L dx$  in Eq. 3, the disturbed medium travel time is:

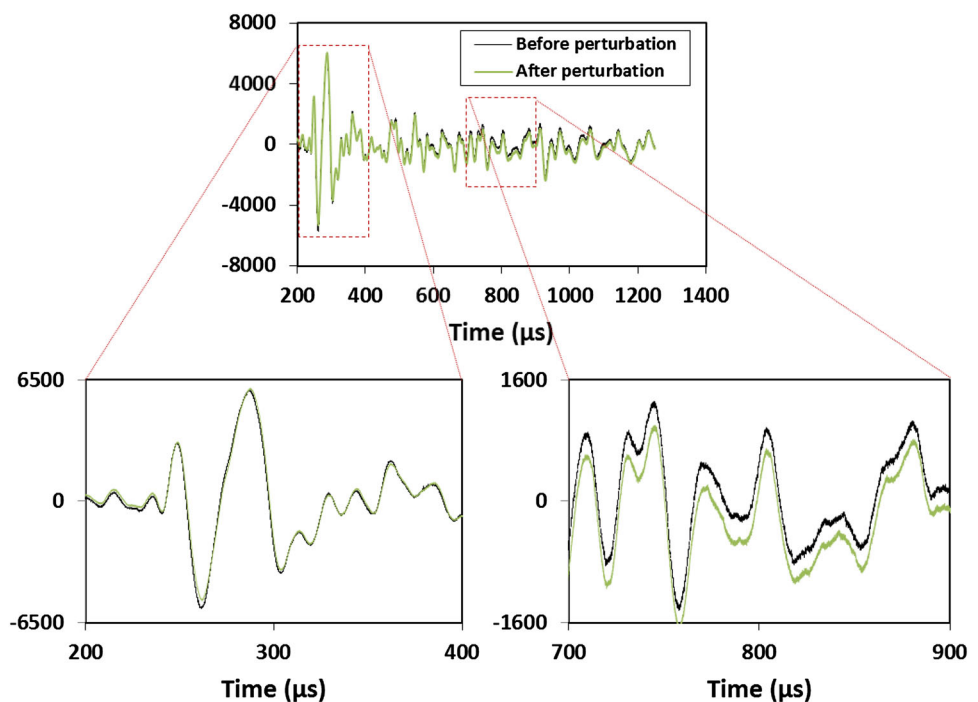
$$\Delta t = -\frac{1}{V_0} \left( \frac{\Delta V}{V_0} \right) \int_L dx = -t_0 \frac{\Delta V}{V_0} \tag{4}$$

Therefore, the relation between relative velocity change  $\Delta V$  and time shift  $\Delta t$  is defined as Eq. 5:

$$\frac{\Delta t}{t_0} = -\frac{\Delta V}{V_0} \tag{5}$$

Hughes and Kelly [15] showed that the NLA properties of materials are proportional to the relative velocity variation. Considering Eq. 5, it is shown that this proportionality can be developed to the relative time shift, as well. Therefore, the nonlinearity of a medium can be characterized by measuring the relative time shift of probe signals as the medium is excited by high amplitudes waves. This nonlinearity can be defined as Eq. 6 [16]:

**Fig. 1** Example of probe signal before and after perturbation



$$\frac{\Delta t}{t_0} = -\frac{\Delta V}{V_0} = \eta \Delta \epsilon \tag{6}$$

where  $\eta$  is an empirical nonlinear elastic parameter of materials; and  $\Delta \epsilon$  is the reversible deformation due to perturbation of the medium by high amplitude impulses. In an ideal one-dimensional medium with direct propagation of probe waves, the empirical parameter  $\eta$  may correspond to the classical nonlinear parameter  $\beta$  [17]. In order to measure the value of the time shift of the probe waves  $\Delta t$ , Bui et al. [13] proposed a methodology similar to that proposed by Snieder et al. [18] for Coda wave interferometry (CWI). Suppose that a highly heterogeneous material is perturbed by high-amplitude waves. The wave field before an external perturbation ( $S_{unp}$ ) can be expressed as  $S_{unp} = \sum_K u_K(t)$ , where  $t$  is the time, and  $u_K(t)$  is the wave that propagates along a path  $K$ . The wave field after perturbation ( $S_{prt}$ ) can be expressed as  $S_{prt} = \sum_K u_K(t - \tau_K)$  along the multiple scattering trajectories  $K$  when the signal is received with time delay ( $\tau_K$ ) [13].

Figure 1 presents the influence of the perturbation on the travel time of the probe waves. As discussed in [13], the mathematical operator of cross-correlation functions (CC) is used to compute the time shift ( $\Delta t$ ) induced between two signals (i.e. signals before and after perturbation).

$$CC_{S_{unp}S_{prt}}(\tau) = \frac{\int_{t-t_w}^{t+t_w} S_{unp}(t')S_{prt}(t' - \tau)dt'}{\sqrt{\int_{t-t_w}^{t+t_w} S_{unp}^2(t') \cdot S_{prt}^2(t')dt'}} \tag{7}$$

Equation 7 is the normalized cross-correlation function between  $S_{unp}$  and  $S_{prt}$  during a  $2t_w$  time interval that is centered at the time  $t$ . When the medium is not perturbed, it is clear that  $S_{unp} = S_{prt}$ . For an excited medium, the time shift  $\Delta t$  is equal to the value of  $\tau$  that maximizes  $CC_{S_{unp}S_{prt}}$ . The time shift values computed using this method can be used as an indicative to quantify the NLA state of materials.

### 3 Experimental Program

#### 3.1 Sampling and Instrumentation

The tests were carried out on a series of reinforced concrete slabs with dimension of  $1.40 \times 0.75 \times 0.3 \text{ m}^3$ . The dimensions were chosen to allow the mobility of the slabs and an adequate surface for performing the test. These slabs can simulate the field condition (bridge deck) in the laboratory. Three reinforced concrete slabs were fabricated: two slabs incorporating ASR aggregate (Spratt limestone [19]) and one incorporating nonreactive aggregates (control specimen). The composition of the concrete for a density of  $2,400 \text{ kg/m}^3$  is given in Table 1. To accelerate the reaction, pellets of NaOH were added to the mixing water of the reactive concrete in order to reach to the total alkali content of 1.25 %  $\text{Na}_2\text{O}_{eq}$  by mass of cement; all concrete slabs went through a 28-day moisture curing at normal temperature. The average compressive strength and the average modulus of elasticity at 28 days were 39.2 MPa and 36.7 GPa for the reactive concrete and 36.5 MPa and 35.9 GPa for the nonreactive one. Demec gauges and internal vibrating wire gauges were used to monitor ASR expansion of the slabs. Three thermocouples were installed inside of each concrete slabs in order to accurately record the internal temperature of the concrete slabs. Figure 2 shows a layout of the instrumentation in the slabs. All concrete slabs were placed in a warm room ( $50 \pm 2 \text{ }^\circ\text{C}$ ) for accelerating the rate of ASR. To keep moisture, the concrete slabs were covered up by ever-saturated blankets and plas-

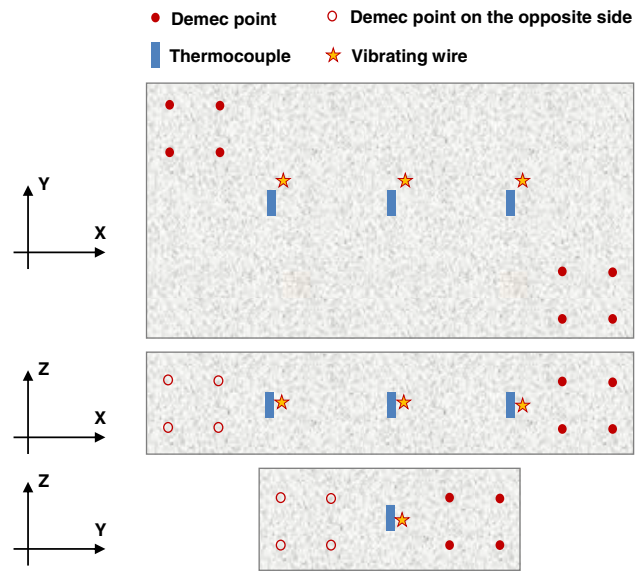


**Fig. 2** Layout of the instrumentation of the concrete slabs. Demec points were installed on the surfaces and the vibrating wires were embedded inside the concrete slabs

tic covers. The concrete slabs were placed in normal ambient condition in order to stabilize the thermal gradient of the concrete slabs. The ASR-expansions were recorded and then, the concrete slabs were moved to a climatic room for performing NDT. This experience was carried out for temperatures between  $-10$  and  $40 \text{ }^\circ\text{C}$  at  $10 \text{ }^\circ\text{C}$  intervals.

#### 3.2 Test Procedure

As the time shift value is directly dependent on the impact energy, an instrumented hammer was used to apply the impacts on the concrete slabs and allowed recording the impact loads. The hammer mass was 3.0 kg with tip diameter of 5.1 cm (impact area  $20 \text{ cm}^2$ ) with maximum load capacity of 22 kN. The maximum frequency of the impacts produced by the hammer is around 1 kHz. In order to obtain more reliable results, the tests were performed with a series of six hammer strikes, regularly from low to high force impulses. The relative time shifts were then normalized to the force impulse because the amplitude of the NLA behavior is linearly proportional to the energy of the force impulse [16, 20, 21]. The normalized values were then averaged out for interpretation. Figure 3 shows the instrumented hammer alongside a series of signals recorded from the hammer impact.

The repeatability of the time shift over exposure time has been previously verified on the nonreactive concrete slab [16]. To do so, five sequences of Time Shift test were carried out on the slab at different levels of impact loadings. The research presented in as previous paper [16] had been performed to verify a methodology for applying the Time Shift method for field investigations.

**Table 1** Mix design of the concrete slabs

Components	Values
Water/cement	0.50
Cement	$400 \text{ kg/m}^3$
Coarse aggregate (5–14mm)	$864 \text{ kg/m}^3$
Coarse aggregate (10–20mm)	$216 \text{ kg/m}^3$
Fine aggregate	$730 \text{ kg/m}^3$
Water	$200 \text{ kg/m}^3$
Total alkali content <sup>a</sup>	1.25 % $\text{Na}_2\text{O}_{eq}$ by mass of cement

<sup>a</sup> Total alkali content: alkali content of cement + alkali content by adding reagent grade NaOH pellets to the mix water

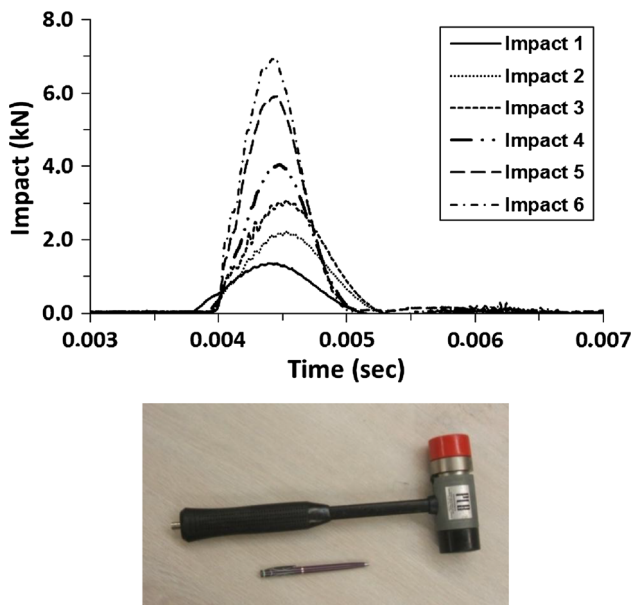


**Fig. 3** Instrumented hammer with the one example of six-step loading

In this paper, the concrete slabs were placed in a controlled temperature room in order to simulate outdoor temperatures for different seasons (between  $-10$  and  $40$  °C at  $10$  °C intervals). This room is large enough for placing the concrete slabs and is equipped with an automatic temperature adjustment facility; it works with temperature limits between  $-15$  and  $50$  °C. For each of temperatures, the tests were carried out after thermal balance in embedded thermocouples.

### 3.3 Data Acquisition and Processing

The vibrations of the slabs due to the hammer strikes were recorded with two piezoelectric accelerometers placed at different parts on the concrete slabs. These accelerometers have a nearly flat response in the frequency range from  $1$  to  $15$  kHz. The acquisition was triggered with the hammer strike and the signals sampled at the rate of  $0.5$  MHz.

For the Time Shift tests, the time delay values are calculated when the probe signals before and after perturbation are compared to the reference probe signal. The probe signals are created from a signal generator and are amplified with an integrated amplifier. These signals excite a Panametrics piezoelectric longitudinal transducer (P-wave transducer) with a central frequency of  $250$  kHz. The signal is detected after the propagation by the similar transducer and is amplified prior to be sent onto the data acquisition system. Moreover, the transducers were sufficiently stable against the dimensional changes due to the temperature variations between  $-10$  and  $40$  °C. The recorded data of the probe wave are digitized at a sampling rate of  $60$  MHz. For each test, the unperturbed signal (before hammer strike) is considered as the reference

signal in the cross-correlation function (Eq. 7). The accuracy of the measurements is in such extent way that the smallest value of  $\Delta t$  processed by the cross-correlation function is in the magnitude of  $0.01$   $\mu$ s. Figure 4 shows a sketch of the test set-up with configuration of piezoelectric accelerometers and transducers, and data acquisition system for the concrete slabs.

To find the maximum value of the time shift, the whole signal was processed with a consecutive time window method. In this method, a time window with a  $100$   $\mu$ s width seeks the recorded signal between  $200$   $\mu$ s and  $1,000$   $\mu$ s with a sweep rate of  $1$   $\mu$ s. The whole length of recorded signal is then processed in order to point out the maximum value of time shift ( $\Delta t_{max}$ ). This seeker time window is assumed to be large enough to take into account enough signal to improve the correlation accuracy. Figure 5 shows a schematic of the moving-window analysis method used in this research.

## 4 Results and Discussion

Length variations were used to evaluate the progression of ASR in the concrete slabs. Figure 6 shows the average expansion curve for the reactive slabs alongside images exhibiting typical symptoms of ASR. The experiment was conducted when the reactive slabs 1 and 2 reached expansion levels of  $0.14$  and  $0.19$  %, respectively.

### 4.1 Perturbation of Concrete Slabs

The Time Shift method likely measures the state of a material after being excited with high-amplitude impulse. The response of the medium to an imposed perturbation depends on the physical properties such as the material stiffness. It should be mentioned that the temperature variations, specifically at low temperatures, influence the stiffness of the concrete, which may directly affects the NLA response. Indeed, the variations of the physical properties of the materials introduce significant changes in their modal vibrations and resonant frequency. Donskoy et al. [20] showed a direct relationship between the NLA response of the materials and their modes of vibration.

The vibrations of the concrete slabs due to the hammer strikes were measured with the accelerometers attached to the concrete slabs in order to qualitatively evaluate the modal properties of each concrete slab when the temperature changes from  $-10$  to  $40$  °C. Figure 7 shows an example of the response of slab 1 to the force impulses measured by accelerometer 2. Both the time-amplitude and the frequency-amplitude curves demonstrate a temperature-dependence behavior for the vibrations of the concrete slabs. This figure shows that the wave forms in time domain were stretched or compressed by the temperature variations. The

**Fig. 4** Test set-up with configuration of measuring instruments. Piezoelectric accelerometers for recording the impulse response of concrete (up) and Time Shift test configuration (down)

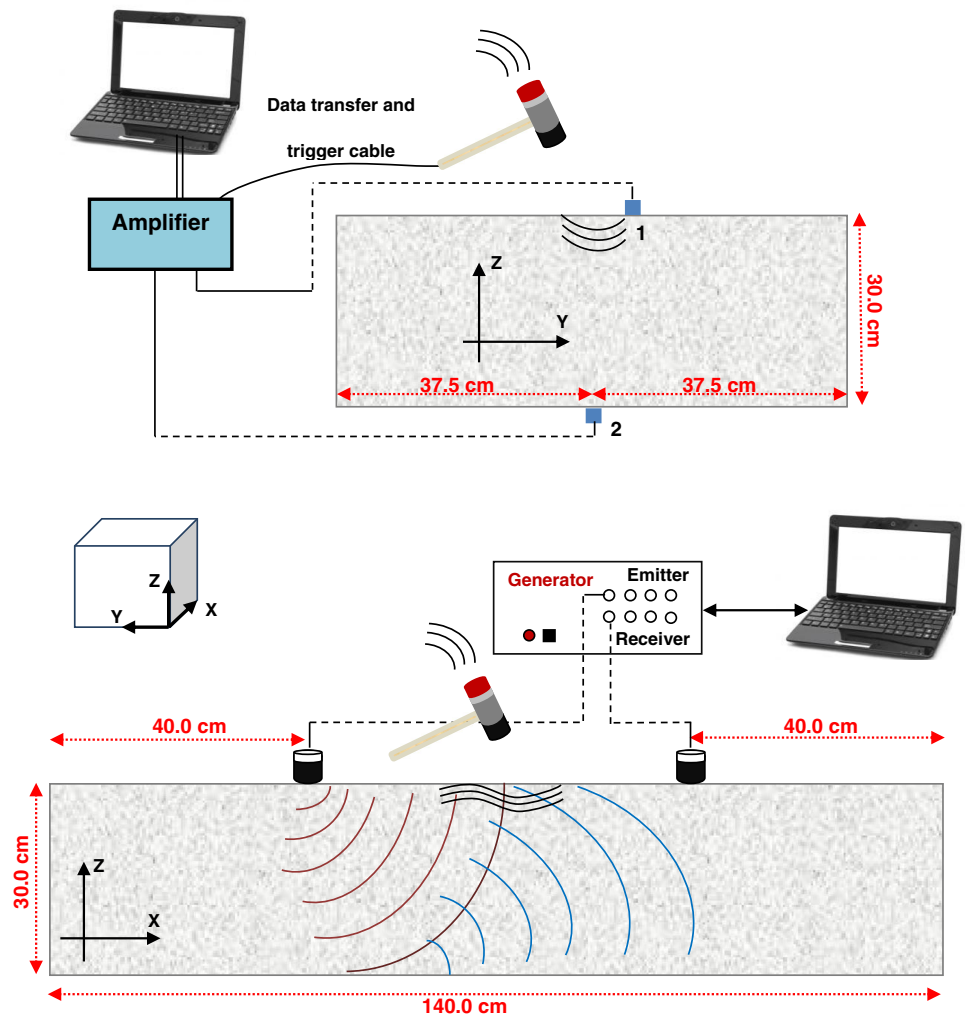
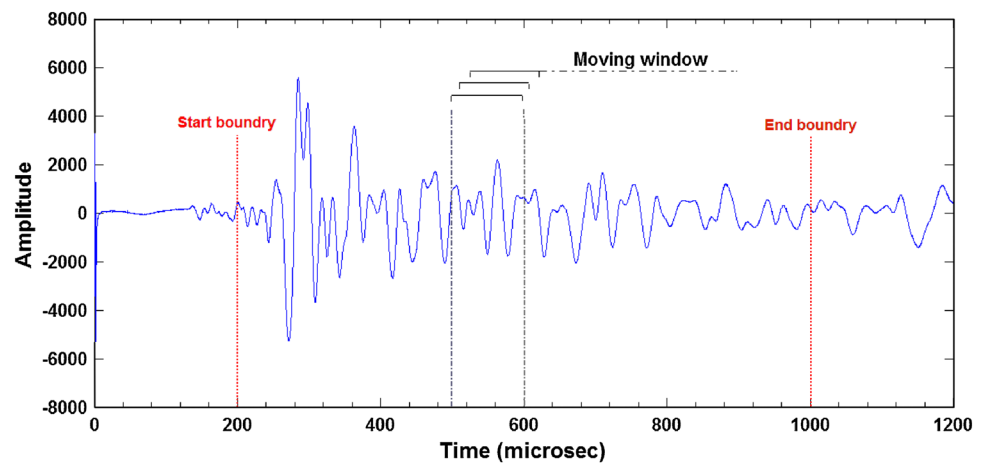


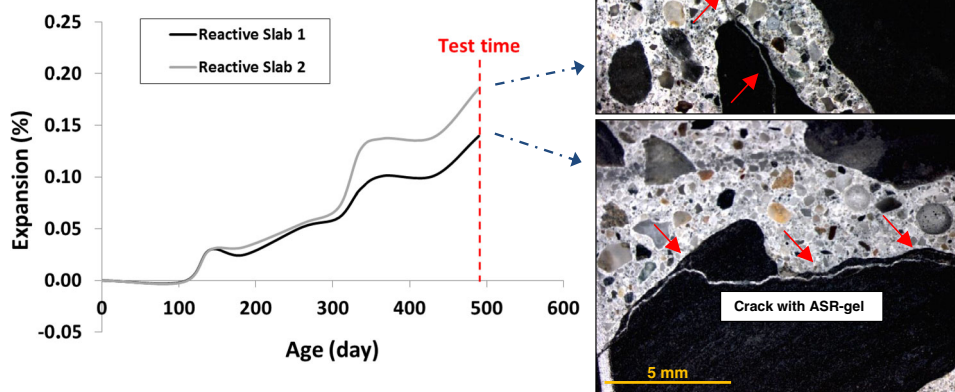
**Fig. 5** Example of recorded signals and a schematic about the method of signal analysis



frequency domain plots show that amplitude of higher frequencies (higher modes of vibration), which mostly correspond to the compressional mode, decreases with temperature increment from  $-10$  to  $40$  °C. The amplitude of the higher frequencies at  $40$  °C becomes negligible. More-

over, the figure shows that the amplitude of lower frequencies (lower modes of vibration), which mostly correspond to flexural mode, generally increases with the temperature arising. In addition to the amplitude variations of higher and lower frequencies, a shift of the resonant frequencies under

**Fig. 6** ASR expansion of the reactive concrete slabs with microscopic images. Test time is marked with a red dash line



temperature changes was observed. These variable spectral properties represent the thermal dependent vibration of the concrete slabs that come from the variations of NLA properties due to the temperature changes.

#### 4.2 Nonlinear Acoustic Assessment

The Time Shift method, as a dynamic acoustoelastic method, was applied to assess the NLA response of the concrete slabs as the temperature changes. The variations of the NLA behavior induced by the temperature were predicted when the variations of the modal properties was observed.

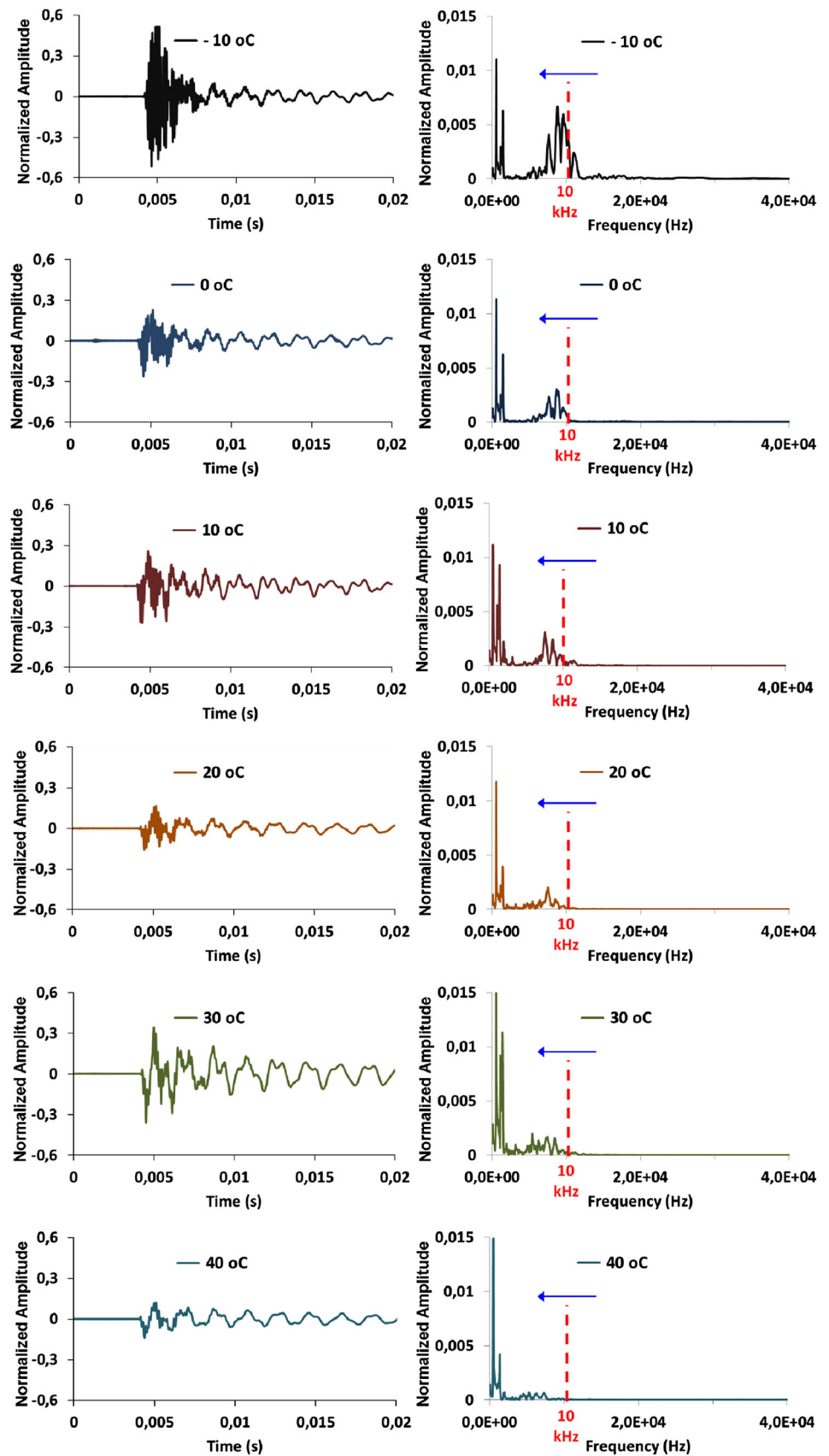
The repeatability of the measurements recorded at ambient temperature ( $20 \pm 2$  °C) was assessed in [16]. The required impact loads was provided with a MTS hydraulic actuator, and the test was repeated for eight-step loadings from 10 to 40 kN with a step-load 5 kN. This method for generating low frequency and high amplitude waves is explained in detail in [14, 16]. Figure 8 shows the  $\Delta t_{max}/t_0$  results measured for the nonreactive slab. The results are fairly stable over time; however, small fluctuation in Time Shift values can be related to some microstructural modifications, humidity changes, ambient temperature variations, possible test errors, etc. The slope coefficients of linear trends vary between 0.0010 and 0.0014. This verification conducted over 360 days allowed concluding that the Time Shift test is repeatable over exposure time at ambient temperature of  $20 \pm 2$  °C. Unlikely acoustoelastic methods that should be validated for thermal bias due to air temperature fluctuation of room in the course of each test [22], the results obtained with Time Shift method are independent of the air temperature variations during the tests. Indeed, the measurements by the Time Shift method are quick in such a way that the effect of the air temperature fluctuations during the tests is negligible. Therefore, there is

no need to apply a thermal bias control technique, like that presented in [22], for eliminating the effects of the temperature changes for the results presented here.

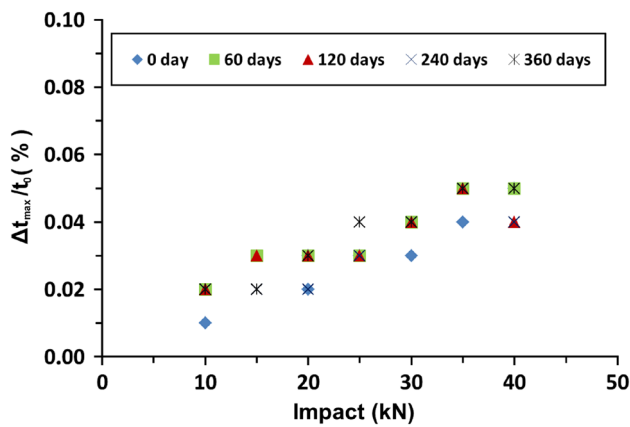
Figure 9 shows the values of normalized maximum recorded  $\Delta t_{max}$  to force impulses in both the reactive and nonreactive slabs. Time Shift technique is generally capable of distinguishing between damaged and sound concrete. However, it is not easy to clearly distinguish the concrete slab with 0.14 % expansion from that with 0.19 % expansion. Overall, this figure may show that acoustoelastic behavior of ASR-damaged concrete is more sensitive to temperature variations than that of sound concrete. This growing trend of  $\Delta t_{max}$  values by temperature variations is originated in concrete stiffness changes with temperature. In other words, even pre-damaged concrete may become stiffer at lower temperatures; whereas the stiffness decreases with increasing temperature.

Figure 10 shows the values of normalized  $\Delta t_{max}/t_0$  to force impulses for the three slabs. The reactive concrete slabs with expansion levels of 0.14 and 0.19 % are clearly distinguishable. As shown in the figure, there is a rising trend between  $\Delta t_{max}/t_0$  and the temperature. The slope of these rising trends represents the extent of the damage in the concrete slabs. In other words, the slope of the rising trends gradually increases from the nonreactive slab to the reactive slabs with the highest expansion (i.e. 0.19 %). In comparison with the nonreactive slab, this slope is by five times higher for the reactive slab with expansion 0.14 % and eight times higher for the reactive slab with expansion 0.19 %. This phenomenon can be related to the higher sensitivity of stiffness of ASR-damaged concrete to temperature changes. This explanation is supported by the model presented in Eq. 1. Therefore, the NLA behavior of ASR-damaged concrete increases with temperature variations.

**Fig. 7** Waveform in time and frequency domain for the accelerometer at position 2 for reactive slab 1 for temperature variations between  $-10$  and  $40$  °C. The values of amplitude have been normalized to hammer strike loadings.







**Fig. 8** Repeatability of ratio of maximum time shift variation for the nonreactive loading when the slab is perturbed by a hydraulic actuator.

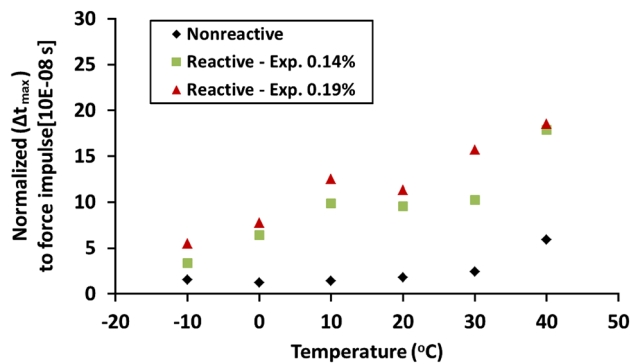


**Fig. 9** Maximum time shift value normalized to the force impulses.

In the meantime, it should be mentioned that the obtained results for the values of  $\Delta t_{max}/t_0$  is in agreement with previous work published by the authors [16]. Indeed, it was shown that the value of  $\Delta t_{max}/t_0$  for an ASR expansion of 0.14 % at a temperature of  $20 \pm 2$  °C was around 0.01 % as the impulse loading was 1 kN. Accordingly, the relative time shift values for the concrete slab with expansion 0.19 % and the nonreactive slab are in agreement with the reference value.

The values of  $\Delta t_{max}/t_0$  at low temperatures are nearly the same, being smaller than those at higher temperatures. These values also show that the difference between sound and ASR-affected concrete at  $-10$  and  $0$  °C is hard to make. As discussed above, the low response of the micro-defects to the perturbation at low temperatures (due to stiffer concrete) can induce the lower values of  $\Delta t_{max}/t_0$ , even in ASR-damaged concrete. The thermal behavior of the concrete depends on its constitutive ingredients, pore and inter-layer water contents, and its by-products (in this case, ASR-gel). The hydraulic pressure theory developed by Powers and Helmuth [23] stipulates that the internal pore pressure can increase by around 9 % during water freezing, and it gradu-

ally causes freezing shrinkage in micro-defects. In the case of ASR-damaged concrete, Larive [24] showed an indirect relationship between viscosity of ASR-gel and exponential of temperature; ASR-gel viscosity increases at lower temperature reduction, which may highly affect the stiffness of internal micro-cracks filled with ASR-gel. This increment of stiffness is in such a manner that no significant difference was observed between sound and ASR-damaged concrete at  $-10$  and  $0$  °C. NLA techniques are based on local modifications of the medium that takes its root from the elastic deformations of the microstructural defects. These local modifications occur when the medium is excited with high amplitude waves. At temperatures lying between  $-10$  and  $0$  °C, either frozen pore water or highly viscous gel may limit the movement of the microstructural defects (primarily the micro-cracks filled with water and/or gel). Therefore, the NLA responses of both the sound and ASR-damaged slabs show about the same behavior.

According to Eq. 1, temperature variations have much more influence on the ASR damaged concrete in comparison with the sound concrete because of much more micro-defects and defects. With increasing temperature, the stiffness of concrete decreases and the micro-defects are more affected by the high amplitude waves. A detailed analysis of the results shows that the  $\Delta t_{max}/t_0$  values increase for the temperature ranging from  $10$  to  $30$  °C in comparison with those measured for the temperatures ranging from  $-10$  to  $0$  °C; this increment is much more intensified for ASR-damaged concrete. However, the variation of the relative Time Shift values is moderated at this temperature range for all specimens, as shown in Fig. 11.

At higher temperatures ( $40$  °C), a sudden increase of  $\Delta t_{max}/t_0$  was observed in both the reactive and nonreactive slabs. Figure 7 also shows important changes for the spectrum density of the vibration of the slabs at a temperature of  $40$  °C. This phenomenon may be associated with the stiffness reduction of the concrete. Therefore, the microstructural defects can experience much more when the medium is perturbed by high amplitude waves. Other factors like the redistribution and the evaporation of moisture from the microstructural pores at higher temperatures may affect NLA behavior of materials. This sudden augmentation of  $\Delta t_{max}/t_0$  is more visible for the ASR-damage concrete. This can be related once again to the ASR-gel viscosity that highly drops at temperatures above  $40$  °C, the gel being more fluid [25]. This reduction of the gel viscosity is also confirmed by Jones and Poole [26], where they observed less expansions for the specimens stored at temperatures above  $40$  °C. The authors inferred that the low viscosity of the gel made it flow freely through the micro-defects and defects without exerting large stresses. Therefore, the NLA response of the ASR-damaged slabs for temperatures above  $40$  °C would be amplified.

**Fig. 10** Relative time shift variations normalized to the force impulses for the concrete slabs

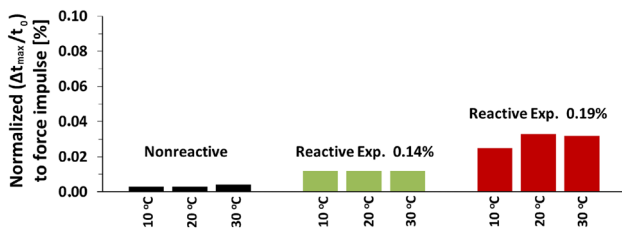
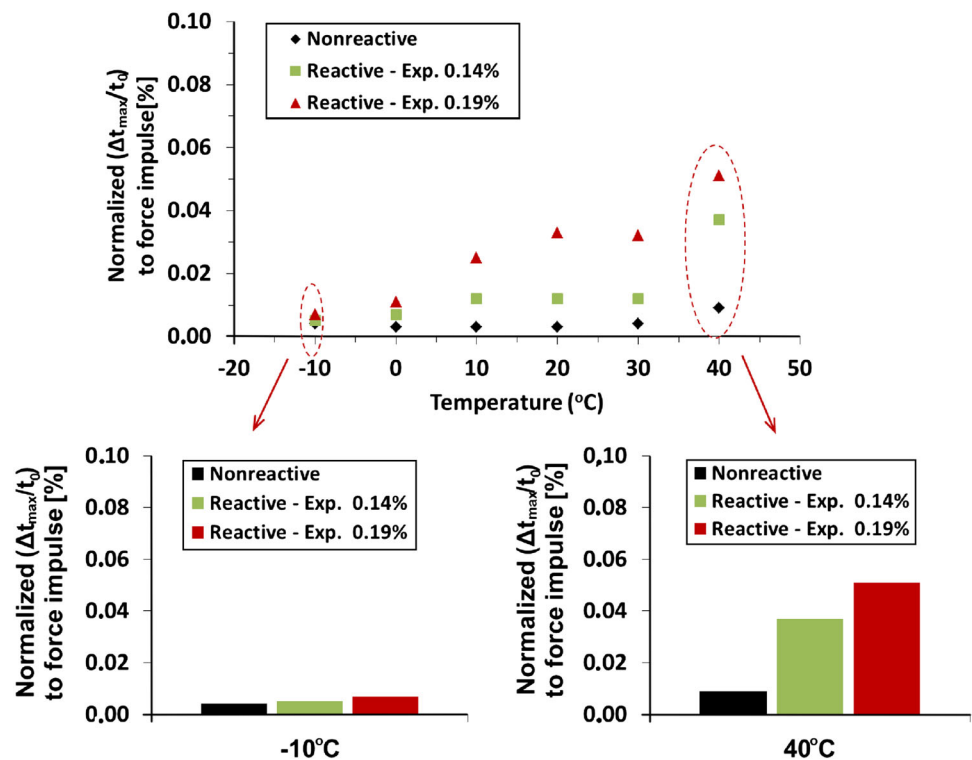


**Fig. 11** Maximum time shift variation normalized to reference for temperatures between 10 and 30 °C.

### 5 Conclusion and Prospects

Despite the fact that NLA methods are potentially suitable for field investigations, the literature review has identified a lack of information on the effects of the environmental parameters (e.g. temperature) on the NLA behavior of the concrete. For fruitful field investigations, there is a need to uncouple between damage and effects of environmental parameters. The method of Time Shift, as a dynamic acoustoelastic method, was used to quantitatively evaluate effects of the temperature variations on the NLA properties of sound and ASR-damaged reinforced concrete. According to this experiment, the following conclusions can be drawn:

- Temperature variations influence the modes of vibration in such a way that the amplitude of higher modes (mode of compression) decreases with increasing temperature, whereas the amplitude of lower modes (mode of flexion)

moderately increases with temperature. Such variations are due to the thermal dependency of the NLA response of the defects to imposed perturbation.

- For temperatures ranging from  $-10$  to  $0$  °C,  $\Delta t_{max}/t_0$  values are negligible in both the sound and ASR-damaged concrete. This observation is associated with higher stiffness of concrete at subfreezing temperatures. Indeed, at such temperatures, the reversible deformations of micro-defects in the concrete slabs are limited due to higher stiffness of the media. This phenomenon induces very low NLA response of the concrete slabs to imposed perturbation. This result demonstrates that NLA methods may lead to underestimate results during field investigations at low temperatures.
- For temperatures between 10 and 30 °C, a slight fluctuation was observed in  $\Delta t_{max}/t_0$  values. More stable results can be derived at this temperature range for the nonreactive slabs. Similar results were also observed for the ASR-damaged slabs, which can be related to more stable behavior of viscous ASR-gel at this temperature range.
- Sudden increase of  $\Delta t_{max}/t_0$  values was observed in both the intact and ASR-damaged concrete slabs at 40 °C. This observation may be related to some changes in the redistribution of moisture between internal defects and inter-grain contacts (i.e. thermal interaction of liquid and solid phases). The evaporation of internal moisture may be another reason. Both phenomena may cause the volume of the concrete to shrink and may induce the capillary

pressure to change. All these discussions should be investigated in future works. For ASR-damaged slabs, sudden decline of ASR-gel viscosity at temperatures above 40 °C can be considered as the main reason for sudden increase of  $\Delta t_{max}/t_0$ .

This research demonstrates that a thermal regime between 10 and 30 °C for performing the NLA testing may lead to more reliable results. For evaluating progress of a damage mechanism such ASR with NLA methods, it is recommended to carry out all tests in a steady temperature at the similar thermal regime (10 and 30 °C). For on-site investigations, obtained results should be analyzed considering the general and microclimatic temperatures of the environment where structures are located.

Future work is underway in an attempt to investigate the relationships between stiffness, modes of vibration and NLA behavior of the concrete.

**Acknowledgments** The authors gratefully acknowledge the financial supports provided by the Natural Science and Engineering Research Council of Canada (NSERC), by the Fonds Québécois de Recherche sur la Nature et les Technologies (FQRNT), by the Federal Highway Administration (FHWA). We also thank Danick Charbonneau, Georges Lalonde and Raphael Prévost for their invaluable technical help.

## References

1. Van Den Abeele, K.E.-A., Sutin, A., Johnson, P.A., Carmeliet, J.: Micro-damage diagnostics using nonlinear elastic wave spectroscopy (NEWS). *NDT & E Int.* **34**, 239–248 (2001)
2. Lesnicki, K.J., Kim, J.Y., Kurtis, K.E., Jacobs, L.J.: Assessment of alkali-silica reaction damage through quantification of concrete nonlinearity. *Mater. Struct.* **46**, 497–509 (2013). doi:10.1617/s11527-012-9942-y
3. Van Den Abeele, K., Visscher, J.D.: Damage assessment in reinforced concrete using spectral and temporal nonlinear vibration techniques. *Cem. Concr. Res.* **30**, 1453–1464 (2000)
4. Vakhnenko, O., Vakhnenko, V., Shankland, T.J.: Soft-ratchet modeling of end-point memory in the nonlinear resonant response of sedimentary rocks. *Phys. Rev. B* **71**, 174103 (2005)
5. Payan, C., Garnier, V., Moysan, J.: Effect of water saturation and porosity on the nonlinear elastic response of concrete. *Cem. Concr. Res.* **40**, 473–476 (2010)
6. Johnson, P.A., Zinszner, B., Rasolofosaon, P., Cohen-Tenoudji, F.: Dynamic measurements of the nonlinear elastic parameter  $\alpha$  in rock under varying conditions. *J. Geophys. Res.* **109**(B02202), 1–12 (2004)
7. Carmeliet, J., Van Den Abeele, K.: Poromechanical approach describing the moisture influence on the non-linear quasi-static and dynamic behaviour of porous building materials. *Mater. Struct.* **37**, 271–280 (2004)
8. Lu, Y., Michaels, J.E.: A methodology for structural health monitoring with diffuse ultrasonic waves in the presence of temperature variations. *Ultrasonics* **43**, 717–731 (2005)
9. Weaver, R.L., Lobkis, O.I.: Temperature dependence of diffuse field phase. *Ultrasonics* **38**, 491–494 (2000)
10. Lobkis, O.I., Weaver, R.L.: Coda-wave interferometry in finite solids: recovery of P-to-S conversion rates in an elastodynamic billiard. *Phys. Rev. Lett.* **90**(254302), 1–4 (2003)
11. Darling, T.W., Ulrich, T.J., Johnson, P.A., TenCate, J.A.: Low temperature elastic constants and nonlinear acoustic response in rocks and complex materials. Los Alamos National Laboratory, LA-UR-01-4484 (2001)
12. Kodjo, A.S.: Contribution à la caractérisation des bétons endommagés par des méthodes de l'acoustique non linéaire. Application à la réaction alcalis-silice Ph.D. thesis in French, Université de Sherbrooke and Université de Cergy-Pontoise, pp. 127 (2008)
13. Bui, D., Kodjo, S.A., Rivard, P., Fournier, B.: Evaluation of concrete distributed cracks by ultrasonic travel time shift under an external mechanical perturbation: Study of indirect and semi-direct transmission configurations. *J. Nondestruct. Eval.* **32**, 25–56 (2013)
14. Moradi-Marani, F., Kodjo, S.A., Rivard, P., Lamarche, C.-P.: Application of the mechanical perturbation produced by traffic as a new approach of nonlinear acoustic technique for detecting microcracks in the concrete: A laboratory simulation. *AIP Conf. Proc.* **1430**, 1493–1499 (2012)
15. Hughes, D.S., Kelly, J.L.: Second-order elastic deformation of solids. *Phys. Rev.* **92**, 1145–1149 (1953)
16. Moradi-Marani, F., Kodjo, S.A., Rivard, P., Lamarche, C.-P.: Nonlinear acoustic technique of Time Shift for evaluation of ASR-damage in concrete structures. Accepted for publication in *ACI Mater. J.* (2014)
17. Schurr, D.P., Kim, J.-Y., Sabra, K.G., Jacobs, L.J.: Damage detection in concrete using coda wave interferometry. *NDT & E Int.* **44**, 728–735 (2011)
18. Snieder, R., Grêt, A., Douma, H., Scales, J.: Coda wave interferometry for estimating nonlinear behavior in seismic velocity. *Science* **295**, 2253–2255 (2002)
19. Rivard, P., Ballivy, G.: Assessment of the expansion related to alkali-silica reaction by the damage rating index method. *Constr. Build. Mater.* **19**, 83–90 (2005)
20. Donskoy, D., Sutin, A., Ekimov, A.: Nonlinear acoustic interaction on contact interfaces and its use for nondestructive testing. *NDT & E Int.* **34**, 231–238 (2008)
21. Chen, X.J., Kim, J.-Y., Kurtis, K.E., Qu, J., Shen, C.W., Jacobs, L.J.: Characterization of progressive microcracking in Portland cement mortar using nonlinear ultrasonics. *NDT & E Int.* **41**, 112–118 (2008)
22. Zhang, Y., Abraham, O., Tournat, V., Le Duff, A., Lascoup, B., Loukili, A., Grondin, F., Durand, O.: Validation of a thermal bias control technique for coda wave interferometry (CWI). *Ultrasonics* **53**, 658–664 (2013)
23. Powers, T.C., Helmuth, R.A.: Theory of volume changes in hardened Portland cement paste during freezing. *Highw. Res. Board. Bull.* **32**, 285–297 (1953)
24. Larive, C.: Apports combinés de l'expérimentation et de la modélisation à la compréhension de l'alcali-réaction et de ses effets mécaniques. PhD thesis in French, École Nationale des Ponts et Chaussées, pp. 327 (1997)
25. Capra, B.: Modélisation des effets mécaniques induits par les réactions alcalis-granulats. PhD thesis in French, École Normale Supérieure de Cachan, pp. 194 (1997)
26. Jones, T.N., Poole, A.B.: Alkali-silica reaction in several UK concretes: the effect of temperature and humidity on expansion, and the significance of ettringite development. In: Proceedings of 7th international conference on alkali-aggregate reaction, Ottawa, Canada (1987)